

GROUND DATA PROCESSING & PRODUCTION OF THE LEVEL 1 HIGH RESOLUTION MAPS



Philippe Rossello

February 2008

CONTENTS

1. Introduction	2
2. Available data	2
2.1. SPOT image	2
2.2. LAI2000 measurements.....	3
2.3. Sampling strategy	4
2.3.1. Principles.....	4
2.3.2. Evaluation based on NDVI values	4
2.3.3. Evaluation based on classification	5
2.3.4. Using convex hulls.....	7
3. Determination of the transfer function for the two biophysical variables: LAI, fCover.....	7
3.1. The transfer function considered.....	7
3.2. Results	8
3.2.1. Choice of the method	8
3.2.2. Choice of the band combination.....	9
3.3. Applying the transfer function to the Järvelja SPOT image extraction.....	12
4. Conclusion.....	13
5. Acknowledgements	13
ANNEX.....	14



1. Introduction

This report describes the production of the high resolution, level 1, biophysical variable maps for the Järvselja site in April 2007 (see campaign report for more details about the site and the ground measurement campaign: annex or <http://www.avignon.inra.fr/valeri>). Level 1 map corresponds to the map derived from the determination of a transfer function between reflectance values of the SPOT image acquired during or around the ground campaign and biophysical variable measurements (LAI2000 in this case).

The derived biophysical variable maps are:

- Leaf Area Index (LAI): LAI corresponds to effective LAI derived from the description of the gap fraction as a function of the view zenith angle;
- cover fraction (fCover): it is the percentage of soil covered by vegetation between 0° and 7° view zenith angle.

The site is a “heterogeneous subboreal forest”. It is mostly covered by a “mixed, uneven aged forest including conifers (Scots pine and Norway spruce) and deciduous (birch, aspen, alder) tree species. There are no agricultural fields in the area, even though a few unmanaged open areas are situated next to the VALERI test site. In the SE and NE parts of the test site there are bogs and mires”. Note that the site is quite flat (for more information, see annex or campaign report: <http://www.avignon.inra.fr/valeri>).

The site coordinates are described in Table 1:

	Lambert-Est-92 WGS-84 (units=meters)		Geographic Lat/Lon WGS-84		UTM 35, North, WGS-84 (units=meters)	
	Easting	Northing	Lat	Lon	Easting	Northing
Upper left corner	689716.0000	6468150.0000	58.31276719	27.23798434	513944.1795	6463556.9852
Lower right corner	692716.0000	6465150.0000	58.28455417	27.28659883	516805.9994	6460426.9088
Center	691216.0000	6466650.0000	58.29866300	27.26230129	515375.0918	6461991.9477

Table 1. Description of the site coordinates: they correspond to SPOT image coordinates.

The ground measurements were carried out from 19th to 25th April 2007, while the high spatial resolution image was acquired in May.

2. Available data

2.1. SPOT image

The SPOT image was acquired the 6th May 2007 by HRVIR1 on SPOT4. The radiometric and geometric correction was performed by SPOT image (product 1B). The image was geo-referenced by TARTU Observatory. The projection is Lambert-Est-92 (Lambert Conformal Conic 2 parallel), WGS-84. Please, refer to the campaign report for more details: annex or <http://www.avignon.inra.fr/valeri>. No atmospheric correction was applied to the image. However, as the SPOT image is used to compute empirical relationships between reflectance and biophysical variable, we can assume that the effect of the atmosphere is the same over the whole 3 x 3 km site. Therefore, it will be taken into account everywhere in the same way.

Figure 1 shows the relationship between Red and near infrared (NIR) SPOT channels: the soil line is marked and no saturated point is observed.

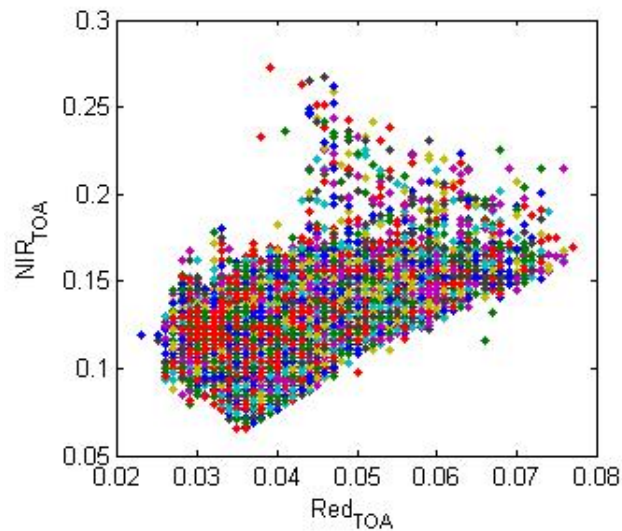


Figure 1. Red/NIR relationship on the SPOT image for Järvelja, 2007

2.2. LAI2000 measurements

For each Elementary Sampling Unit (ESU), the biophysical variables (LAI, fCover) were derived from LAI2000 instrument. The measurements were made at breast height. According to the sampling protocol (annex or <http://www.avignon.inra.fr/valeri>), 48 measurements were taken for each ESU. The ESU biophysical variables that are used in the following were computed as:

- LAI = LAI_canopy
- fCover is the percentage of soil covered by vegetation at 7° view zenith angle.

Figure 2 shows the distribution of the different measured variables over the sampled ESUs. LAI varies from 0.65 to 3.48 and fCover from 0.189 to 0.899. This range shows a heterogeneous site in terms of LAI.

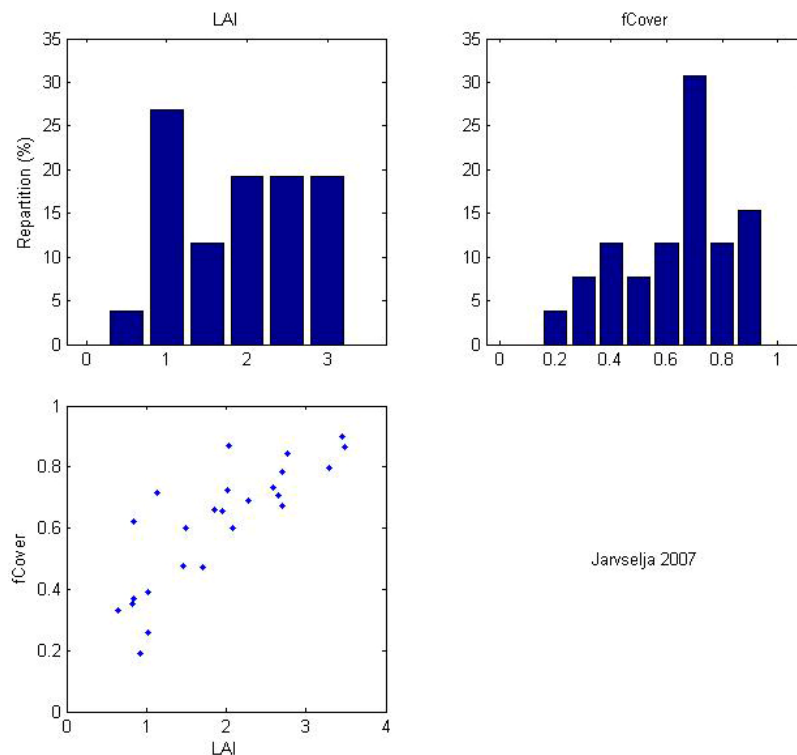


Figure 2. Distribution of the measured biophysical variables over the ESUs.



2.3. Sampling strategy

2.3.1. Principles

The sampling strategy is defined in the campaign report: <http://www.avignon.inra.fr/valeri>. It was attempting to represent as much as possible the range of variation of canopy types and conditions.

Figure 3 shows that the 26 ESUs are evenly distributed over the site (3 x 3 km). The processing of the ground data has shown that: considering that SPOT geo-location and GPS measurements are associated to errors, we found that E2214 and E3107 were too close to the road: they have been shifted by 1 pixel.

Finally, all the ESUs have been kept for the computation of the transfer function:

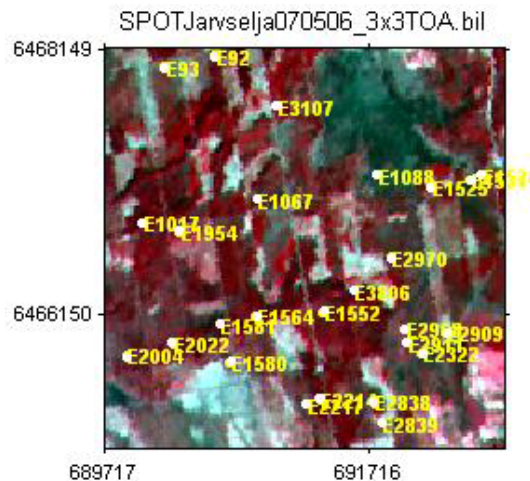


Figure 3. Distribution of the ESUs around the Järvelja site.

2.3.2. Evaluation based on NDVI values

The sampling strategy is evaluated using the SPOT image by comparing the NDVI distribution over the site with the NDVI distribution over the ESUs (Figure 4). As the number of pixels is drastically different for the ESU and whole site ($WS = 22500$ in case of a 3 x 3 km image at 20 m resolution), it is not statistically consistent to directly compare the two NDVI histograms. Therefore, the proposed technique consists in comparing the NDVI cumulative frequency of the two distributions by a Monte-Carlo procedure which aims at comparing the actual frequency to randomly shifted sampling patterns. It consists in:

1. computing the cumulative frequency of the N pixel NDVI that correspond to the exact ESU locations;
2. then, applying a unique random translation to the sampling design (modulo the size of the image);
3. computing the cumulative frequency of NDVI on the randomly shifted sampling design;
4. repeating steps 2 and 3, 199 times with 199 different random translation vectors.

This provides a total population of $N = 199 + 1$ (actual) cumulative frequency on which a statistical test at acceptance probability $1 - \alpha = 95\%$ is applied: for a given NDVI level, if the actual ESU density function is between two limits defined by the $N\alpha/2 = 5$ highest and lowest values of the 200 cumulative frequencies, the hypothesis assuming that WS and ESU NDVI distributions are equivalent is accepted, otherwise it is rejected.

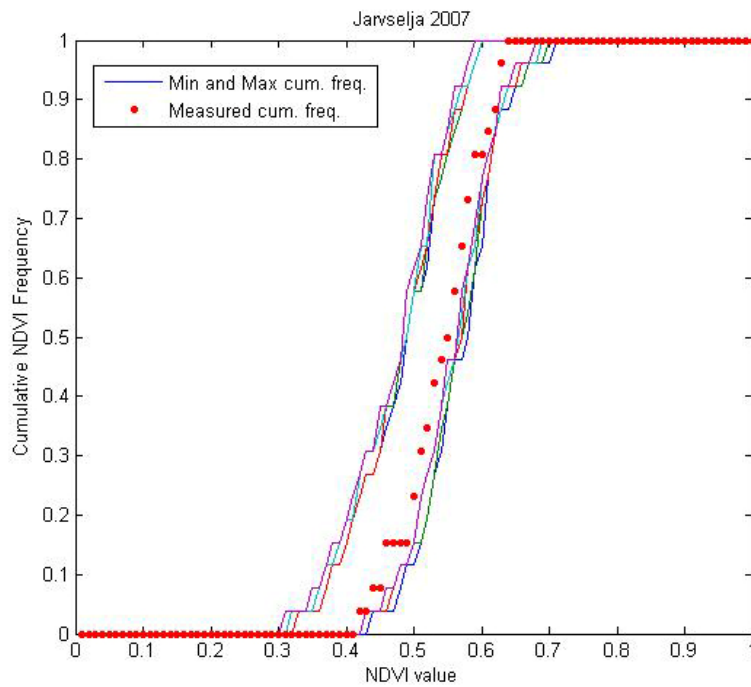


Figure 4. Comparison of the ESU NDVI distribution and the NDVI distribution over the whole image.

Figure 4 shows that the NDVI distribution of the 26 ESUs is good over the whole site even if the cumulative frequency curve is relatively close to the boundaries. Note that NDVIs lower than 0.42 and higher than 0.64 have not been sampled although they are present in the image. They may correspond to paths, recent clear cuts, open areas, agricultural fields...

2.3.3. Evaluation based on classification

A non supervised classification based on the *k*_means method (Matlab statistics toolbox) was applied to the reflectance of the SPOT image to distinguish if different behaviours on the image for the biophysical variable-reflectance relationship exist.

A number of 4 classes was chosen (Figure 5). The distribution of the classes on the image and on the ESUs is rather similar. The classes 3 and 4 are under-represented, while the classes 1 and 2 appear to be over-sampled.

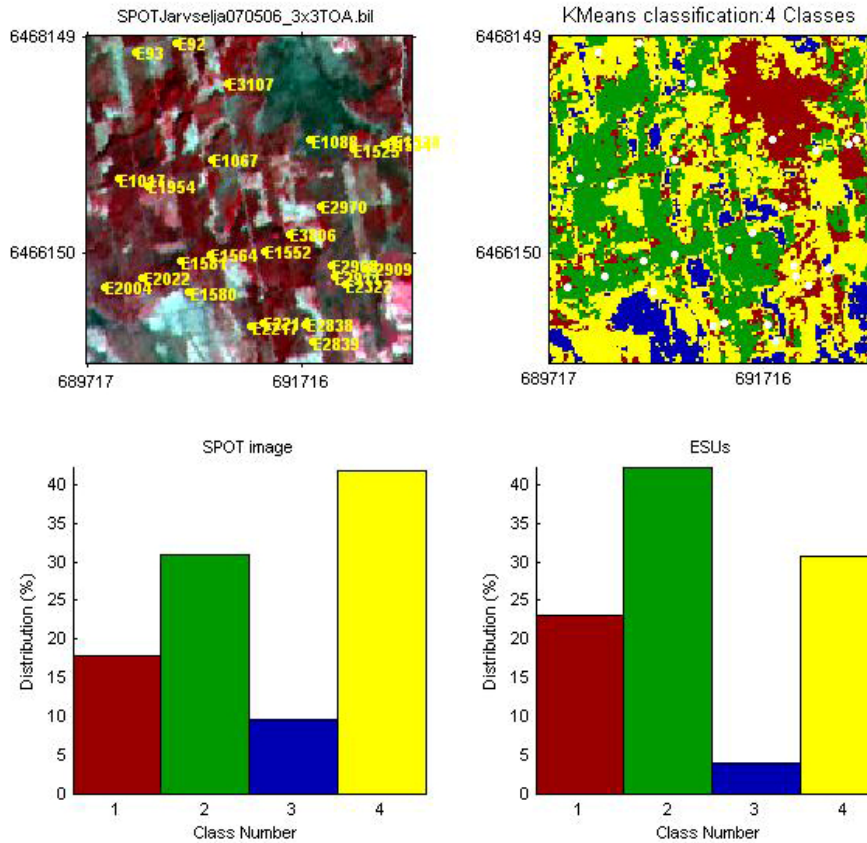


Figure 5. Classification of the SPOT image and comparison of the class distribution between the satellite image and sampled ESUs.

Figure 6 shows the different relationships observed between the biophysical variables and the corresponding NDVI on the ESUs, as a function of the SPOT classes determined from non supervised classification.

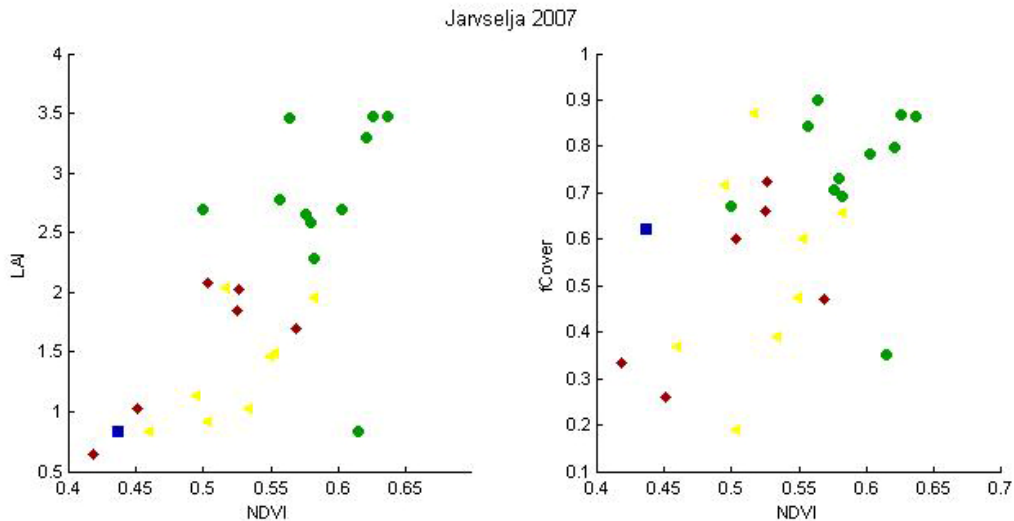


Figure 6. NDVI-biophysical variable relationships as a function of SPOT classes

The relationship between NDVI and biophysical variables is not very good (especially NDVI and fCover). Note that class 3 is only represented by one ESU. No different behaviour between the classes can be observed. Even if the NDVI-biophysical variable relationships are not optimal, a single transfer functions will be generated since the results are satisfactory.



2.3.4. Using convex hulls

A test based on the convex hulls was also carried out to characterize the representativeness of ESUs. Whereas the evaluation based on NDVI values uses two bands (red and NIR), this test uses the 4 bands (green, red and NIR, SWIR in this case) of the SPOT image. A flag image, is computing over the reflectances (Figure 7). The result on convex-hulls can be interpreted as:

- pixels inside the 'strict convex-hull': a convex-hull is computed using all the SPOT reflectance corresponding to the ESUs belonging to the class. These pixels are well represented by the ground sampling and therefore, when applying a transfer function the degree of confidence in the results will be quite high, since the transfer function will be used as an interpolator;
- pixels inside the 'large convex-hull': a convex-hull is computed using all the reflectance combination ($\pm 5\%$ in relative value) corresponding to the ESUs. For these pixels, the degree of confidence in the obtained results will be quite good, since the transfer function is used as an extrapolator (but not far from interpolator);
- pixels outside the two convex-hulls: this means that for these pixels, the transfer function will behave as an extrapolator which makes the results less reliable. However, having a priori information on the site may help to evaluate the extrapolation capacities of the transfer function.

Convex-Hull test for sampling strategy : Jarvselja 2007

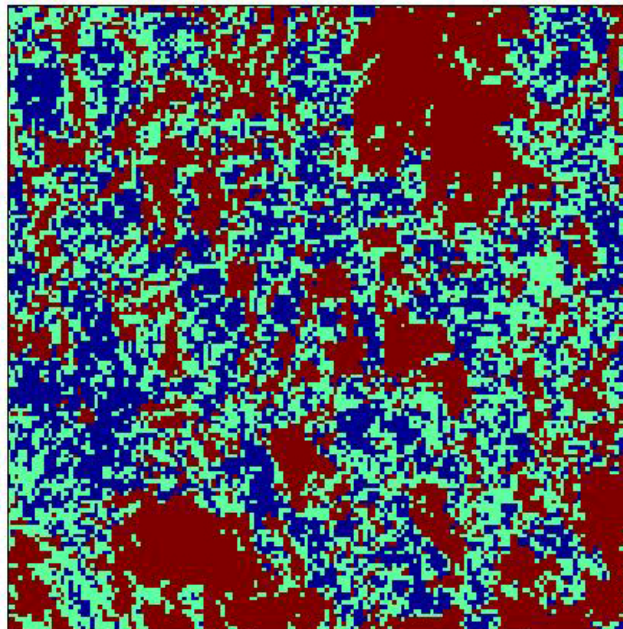


Figure 7. Evaluation of the sampling based on the convex hulls. The map is shown at the bottom: blue and light blue correspond to the pixels belonging to the 'strict' and 'large' convex hulls and red to the pixels for which the transfer function is extrapolating.

The flag map shows that the representativeness of the ESUs is not very good, since numerous pixels are outside the two convex-hulls. They mainly correspond to bogs and mires, recent clear cuts, open areas, agricultural fields...

3. Determination of the transfer function for the two biophysical variables: LAI, fCover

3.1. The transfer function considered

Two types of transfer functions are usually tested in the frame of the VALERI project:

- AVE: if the number of ESUs belonging to the class is too low. The transfer function consists only in attributing the average value of the biophysical variable measured on the class to each pixel of the SPOT image belonging to the class;



- REG: if the number of ESUs is sufficient, multiple robust regression between ESUs reflectance (or Simple Ratio) and the considered biophysical variable can be applied: we used the ‘robustfit’ function from the Matlab statistics toolbox. It uses an iteratively re-weighted least squares algorithm, with the weights at each iteration computed by applying the bisquare function to the residuals from the previous iteration. This algorithm provides lower weight to ESUs that do not fit well. The results are less sensitive to outliers in the data as compared with ordinary least squares regression. At the end of the processing, three errors are computed: classical root mean square error (RMSE), weighted RMSE (using the weights attributed to each ESU) and cross-validation RMSE (leave-one-out method).

For all the classes, the ‘REG’ function is tested using either the reflectance or the logarithm of the reflectance for any band combination as well as the simple ratio or NDVI. As the method has poor extrapolation capacities, a flag image, based on the convex hulls is computing over reflectances.

3.2. Results

3.2.1. Choice of the method

For all the ESUs, a single transfer function is computed. Figure 8 shows the results obtained for all the possible band combinations using either the reflectance (ρ) or the logarithm of the reflectance ($\log(\rho)$): even if the regression made on the $\log(\rho)$ provides slightly better results, the results using the reflectance are selected for LAI and fCover. The transfer function using the $\log(\rho)$ indeed creates coplanar points which do not allow the determination of the ‘strict’ and ‘large’ convex hulls. As the NDVI values corresponding to ground measurements on the Järvelja site are between 0.42 and 0.64, the multi-linear regression is valid only for NDVI ranging between these two values. The extrapolation capacity of this relationship may not be good in certain conditions. Indeed, when applying the relationship on a few pixels in the image, the regression provides a few very high values. As these pixels correspond to high NDVI values, the following values were attributed: LAI = 6 and fCover = 0.95. However, their weight is minimal on the scale to the site.

The Red*NIR (+ or RN) combination is added to all the band combinations (except NDVI and SR). Please read the document (http://www.avignon.inra.fr/valeri/table_methods/new_linear.pdf): “A method to improve the relation between the biophysical variables”.

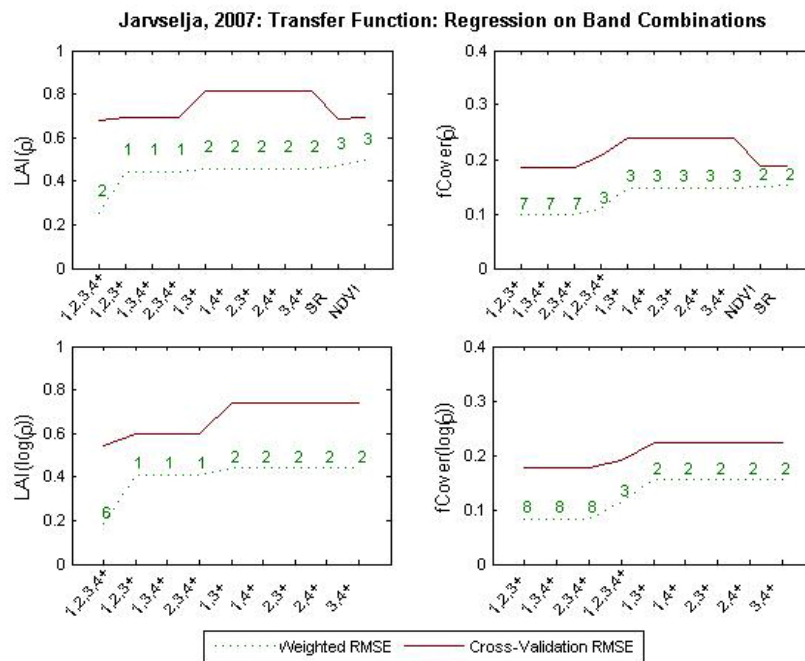


Figure 8. Transfer function: test of multiple regression applied on different band combinations. Band combinations are given in abscissa. The estimated biophysical variable is given in ordinate. Top graphs correspond to regression made on reflectance (ρ): the weighted root mean square error (RMSE) is presented in green along with the cross-validation RMSE in red. The numbers indicate the number of data used for the robust regression with a weight lower than 0.7 that could be considered as outliers. Bottom graphs correspond to regression made on the logarithm of the reflectance.



3.2.2. Choice of the band combination

For the LAI_{eff}, the XS1, XS2, XS3, XS4, RN combination on reflectance (Figure 9 and Figure 10) was selected since it provides a good compromise between the cross-validation RMSE, the weighted RMSE (lowest values), the RMSE and the number of weights lower than 0.7.

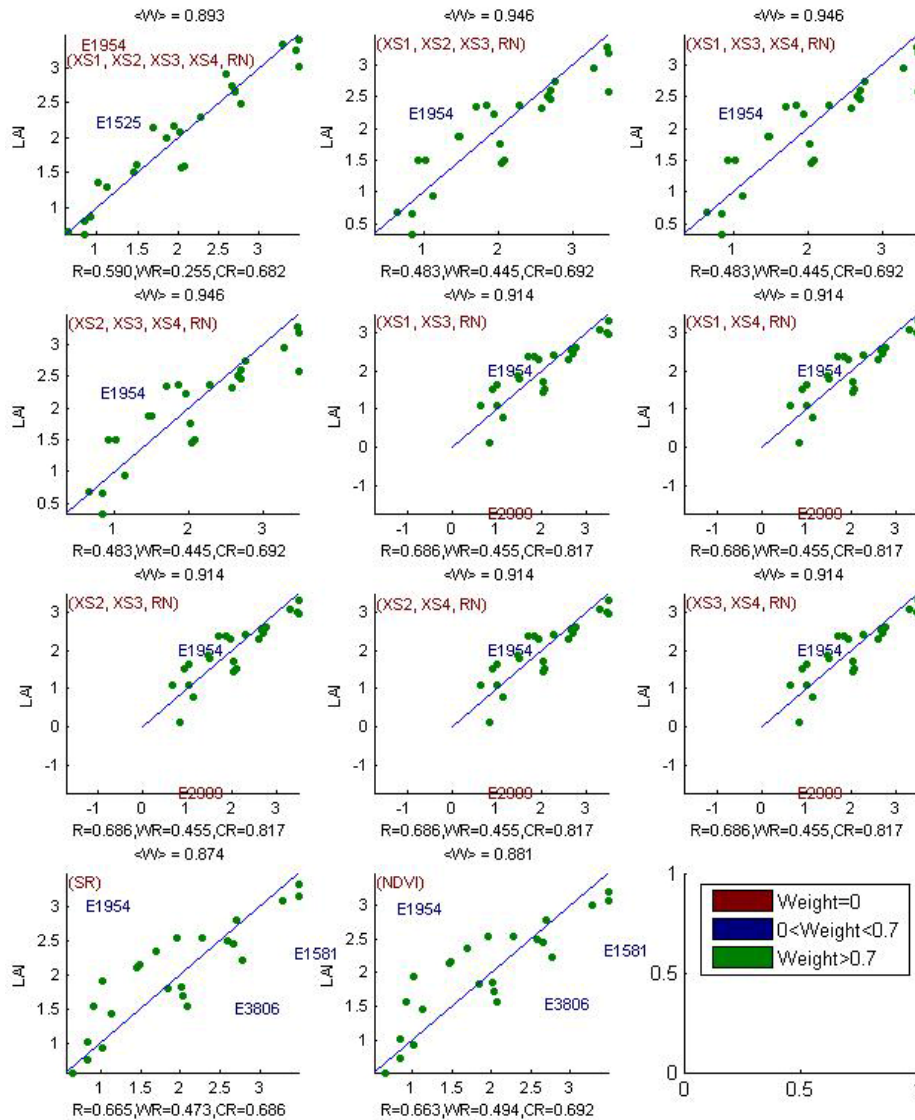


Figure 9. Leaf Area Index: results for regression on reflectance using different band combinations. R is the root mean square error computed between LAI and estimated LAI. WR is the weighted root mean square error and CR is the cross validation root mean square error.

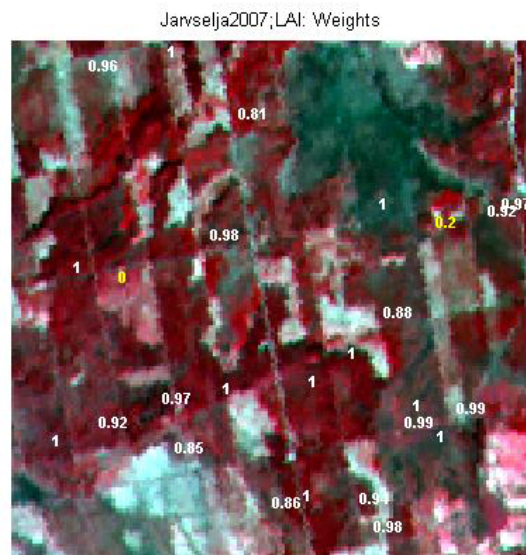


Figure 10. Weights associated to each ESU for the determination of LAI transfer function.

For the fCover, the XS1, XS2, XS3, XS4, RN combination on reflectance (Figure 11 and Figure 12) was selected since it provides a good compromise between the cross-validation RMSE, the weighted RMSE, the RMSE and the number of weights (3) lower than 0.7.



Following, the results of the transfer function (Table 2):

Variable	Band Combination	RMSE	Weighted RMSE	Cross-valid RMSE
LAI	$14.0097 + 74.2351(XS1) - 420.5144(XS2) - 75.9113(XS3) - 28.4367(XS4) + 2896.785(RN)$	0.590	0.255	0.682
fCover	$2.8655 + 25.6236(XS1) - 95.1574(XS2) - 17.9042(XS3) - 6.7288(XS4) + 706.0649(RN)$	0.179	0.108	0.205

RN = Red*NIR

Table 2. Transfer function applied to the whole site for LAI and fCover and corresponding errors

3.3. Applying the transfer function to the Järvelja SPOT image extraction

Figure 13 presents the biophysical variable maps obtained with the transfer function described in Table 2 for all the classes. The maps obtained for the two variables are consistent, showing similar patterns: low LAI values where low fCover are observed and conversely...

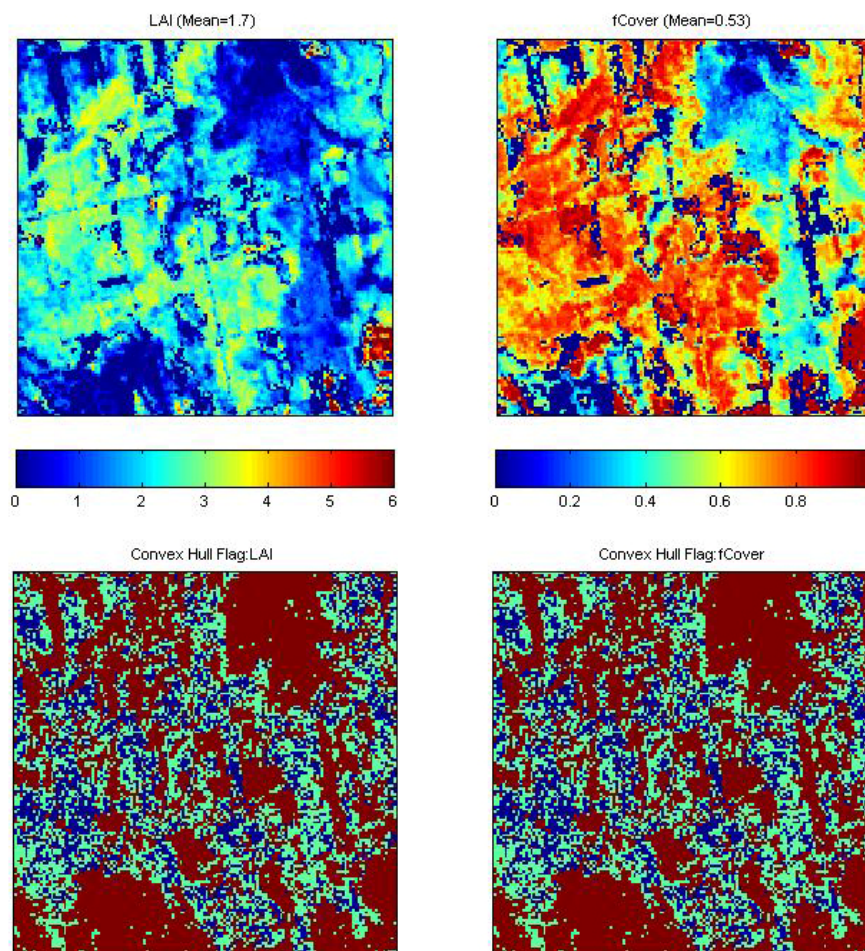


Figure 13. High resolution biophysical variable maps applied on the Järvelja site (top). Associated Flags are shown at the bottom: blue and light blue correspond to the pixels belonging to the ‘strict’ and ‘large’ convex hulls and red to the pixels for which the transfer function is extrapolating

The flag maps are comparable between the two biophysical variables. The pixels outside the two convex-hulls mainly correspond to bogs and mires, recent clear cuts, agricultural fields, open areas (§2.3.4)... Note that the extrapolation is relatively large. In theory, the more the number of bands increases, the larger the extrapolation is.



4. Conclusion

The Järvelja site is heterogeneous in terms of LAI. The representativeness of the land cover of the different ESUs is rather satisfactory. The 'REG' method (§3.1) is applied to all the classes. The results of the robust regression are good and the maps obtained for the biophysical variables are consistent. The flag associated to each map shows that the extrapolation of the transfer function is mainly bounded to bogs and mires, recent clear cuts, agricultural fields... For LAI and fCover, the regression coefficients are computed by relating the variable itself to reflectance.

The biophysical variable maps are available in Lambert-Est-92 (datum: WGS-84) projection coordinates at 20m resolution.

5. Acknowledgements

We want to thank: **Miina Rautiainen**, **Matti Möttus**, **Tiit Nilson** (Tartu Observatory) and **Mait Lang** (Tartu Observatory / University Estonian University of Life Sciences) for the organisation and participation to the campaign.



ANNEX



Ground measurement acquisition report for the VALERI site **Järvelja**

sampled 19-25.04.2007

Organization: Tartu Observatory
email: nilson@aai.ee, miina.rautiainen@helsinki.fi

Date of report 02.05.2007

People participating in planning and field work:

Name	Organization
Miina Rautiainen	Tartu Observatory
Tiit Nilson	Tartu Observatory
Matti Mõttus	Tartu Observatory
Mait Lang	Tartu Observatory / Estonian Univ. of Life Sciences

Site coordinates

	Lat-Long WGS84 (Deg min.00)		UTM / WGS84 UTM		Other projection* Lambert Est 1992	
	Lat.	Long.	Easting	Northing	Easting	Northing
Upper left corner	27 14.28408	58 18.76428	513949	6463554	689721	6468147
Lower right corner	27 17.20086	58 17.07156	516811	6460423	692721	6465147

*The other projection used is LambertEst 1992. All the characteristics are provided in the following table.

Geodesic Map Datum		Map Projection	
Associated Ellipsoid	WGS-84	Latitude of origin	57.51755393055 N
Semi-major axe	6 378 137	Longitude of origin	24.00 E
Semi-minor axe	6 356 752.3	Parallels:	1st
1/flattening	298.257 223 563		2nd
Eccentricity	0.081819190842622	Xo: false easting	500000
		Yo: false northing	6375000
		Scale factor	1

Ground control points

Control points were located from 1:50000 digital map of Estonia. Coordinate system used: LambertEst 1992.

Description of the site and land cover

Comments on the land cover

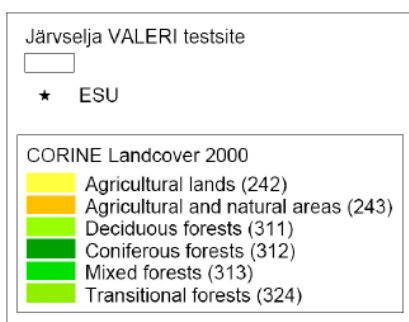
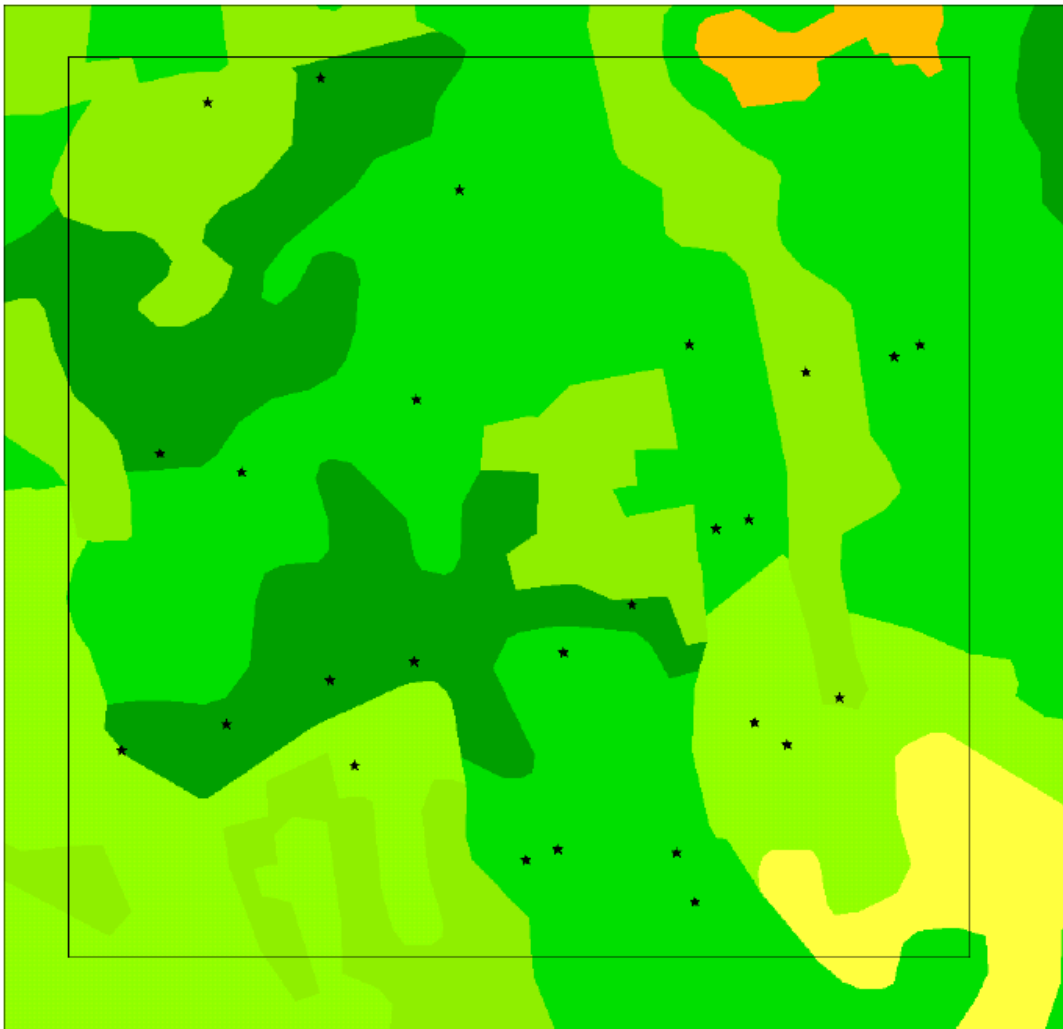
Heterogeneous subboreal forest.

This site is mostly covered by a mixed, uneven aged forest including conifers (Scots pine and Norway spruce) and deciduous (birch, aspen, alder) tree species. There are no agricultural fields in the area, even though a few unmanaged open areas are situated next to the VALERI test site. In the SE and NE parts of the test site there are bogs and mires.

Topography

Flat.

Land cover map

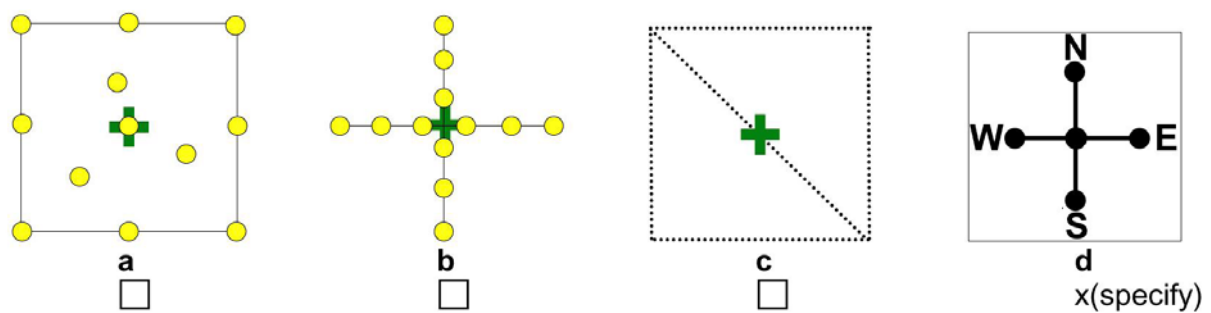


Spatial Sampling scheme

Sensors used for sampling the ESUs

	Method	Comments
<input type="checkbox"/>	Hemispherical photographs	
<input checked="" type="checkbox"/>	LAI-2000	Below canopy (height ca 1m)
<input type="checkbox"/>	TRAC	
<input type="checkbox"/>	Ceptometer	
<input type="checkbox"/>	Direct measurements	
<input type="checkbox"/>	Other	

Sampling strategy for the ESU



Sampling strategy B was used (i.e. 12 points in a cross, 4 meters distance between points).

Distribution of the Elementary sampling units

Please see landcover map.

List of the ESUs

ESU # (pol_id_2001)	Easting*	Northing*	Brief Description
1017	690024	6466829	Dense spruce stand, 40 yrs
1067	690877	6467004	Spruce, 38 yrs
1088	691785	6467188	Mixed alder and birch stand, 45 yrs
1954	690294	6466764	Spruce stand, 20 yrs
2968	691984	6466604	Alder stand, 65 yrs
2970	691877	6466576	Mixed alder and birch stand, 60 yrs
1525	692176	6467098	Mixed spruce and birch stand, 20 yrs
1531	692471	6467149	Flooded birch stand, 45 yrs
1528	692554	6467188	Birch (50 yrs) with a dense spruce understory
2004	689896	6465837	Birch stand, 45 yrs
2022	690245	6465922	Birch (40 yrs) with spruce understory
1581	690592	6466071	Pine stand, 175 yrs
1580	690673	6465785	Birch stands, 35 yrs
1564	690870	6466134	Birch stand (45 yrs) with spruce understory
1552	691369	6466162	Mixed birch and alder stand, 30 yrs
3806	691598	6466323	Old, mixed coniferous stand
2911	692005	6465930	Birch stand (25 yrs)
2909	692288	6466010	Alder stand, 5 yrs
2217	691245	6465470	Birch stand, 50 yrs
2214	691348	6465508	Spruce stand, 45 yrs
2838	691745	6465494	Mixed birch and alder stand, 65 yrs
2839	691807	6465331	Thinned alder stand, 10 yrs
2322	692112	6465856	Alder stand, 40 yrs
93	690184	6467996	Birch stand, 10 yrs
92	690560	6468079	Pine stand, 85 yrs
3107	691020	6467704	Spruce stand, 22 yrs

*Lambert-Est 1992

Photo gallery

Jarvselja1.jpg Jarvselja6.jpg